NANO LETTERS

2009
Vol. 9, No. 8
2961-2966

Growing a Carbon Nanotube Atom by Atom: "And Yet It Does Turn"

Mickaël Marchand,† Catherine Journet,† Dominique Guillot,† Jean-Michel Benoit,† Boris I. Yakobson,‡ and Stephen T. Purcell*,†

Laboratoire de Physique de la Matière Condensée et Nanostructures, Université Lyon 1, CNRS, UMR 5586, Domaine Scientifique de la Doua, F-69622 Villeurbanne cedex, France, and Richard E. Smalley Institute for Nanoscale Science and Technology and Department of Mechanical Engineering and Materials Science, Rice University, Houston, Texas 77005-1892

Received April 30, 2009; Revised Manuscript Received June 11, 2009

ABSTRACT

We use field emission microscopy (FEM) to observe directly the growths of individual carbon nanotubes (CNTs) from the nucleation stage and discover that the CNTs often rotate axially during growth, thus supporting a recently proposed "screw-dislocation-like" (SDL) model. One particularly revealing case is emphasized here in which the CNT turned ~180 times during its 11 min growth. Even more remarkable is the frame-by-frame analysis of the video which shows that the rotation proceeds by discrete steps with about ~24 per rotation, half the number of atoms on the circumferences of common single wall carbon nanotubes (SWNTs). The conclusion is that we directly observed the SDL growth of a SWNT one carbon dimer at a time. This observation should aid researchers to precisely understand and control the growth of SWNTs.

The key issue for realizing the potential of carbon nanotubes (CNTs) has always been, and still remains, better control of CNT growth.[1,2] Measurement techniques, models, and controls are needed at the atomic scale as this is the size of the critical growth zone. Simulations suggest such models,[3,4] but the many possibilities they open must be guided by experiment. Though important progress is now being made by growing CNTs in transmission electron microscopes (TEM),[5−8] they do not yet show how individual atoms integrate into a growing CNT. Drawing on older work for crystals,[9] Ding et al.[10] have recently proposed that atoms may integrate repetitively around the edges of growing single wall nanotubes (SWNTs) by a "screw-dislocation-like" (SDL) mechanism. Such a mechanism is attractive because it points toward controlled growth as currently done in bulk single crystal growth and molecular beam epitaxy and connects the growth speed to helicity because it determines the number of carbon acceptor sites at the growing edge. However to test this theory and find the experimental conditions over which it is applicable, an experimental method that can measure growth with an atomic resolution is needed. In this article we show that field emission permits such resolution and we use it to show that the SDL mechanism in certain conditions can govern SWNT growth.

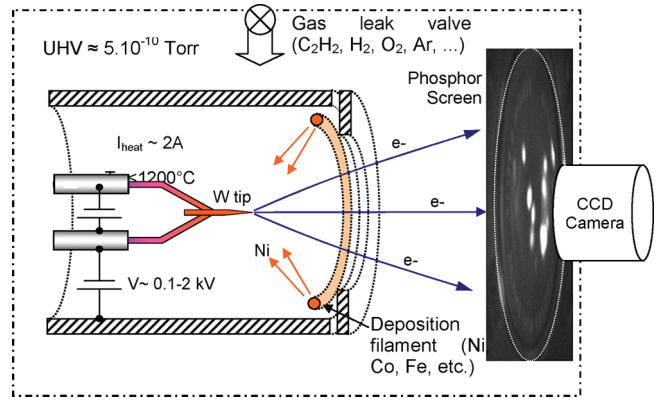

Figure 1. Experimental setup for CNT growth in a FEM.

We grow CNTs by chemical vapor deposition (CVD) on a sharp tip within a field emission microscope (FEM).[11] A schematic of the experimental setup is shown in Figure 1. CNTs are induced to emit electrons from individual CNT caps onto a viewing screen while they grow, including the nucleation phase. The FEM patterns formed on the viewing screen were filmed at standard video speed (25 images/s giving 40 ms per image). This use of FEM was explored in the late 1950s to make direct observations of the growth of single crystal whiskers[11] and recently by Bonard et al.[12] to observe the growth of multiwall CNTs (MWNTs). In these cases the growths were on surfaces with much larger radii of curvature which excluded FEM observation of the nucleation and early growth stages because of the extremely

* Corresponding author, stephen.purcell@lpmcn.univ-lyon1.fr.
† Université Lyon 1.
‡ Rice University.

10.1021/nl901380u CCC: $40.75
Published on Web 07/15/2009

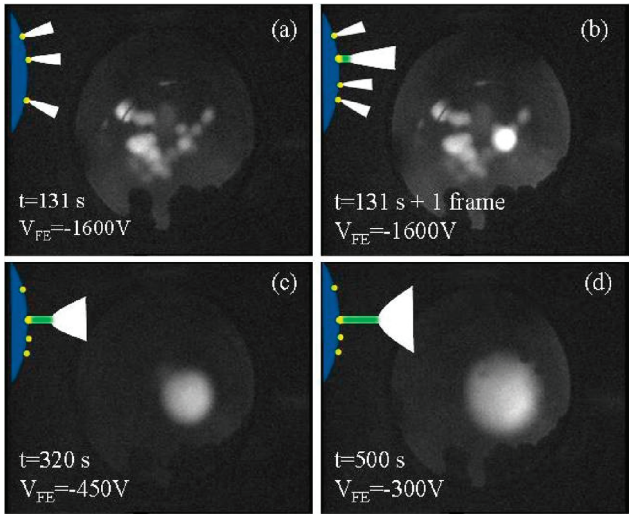

Figure 2. Evolution of the FEM pattern with time during CNT growth in acetylene at 800 °C. (a) FEM pattern from Ni particles before acetylene. Each spot is emission from one Ni nanoparticle. (b) FEM pattern showing a bright circular spot one frame after the CNT nucleation. (c, d) Enlarging CNT-FEM pattern as the CNT lengthens. The voltage has been lowered so that there is no longer any emission from the Ni particles.

high voltages that would have been needed for emission. In our case an electrochemically etched sharp W tip is first spot-welded onto a wire heating loop and placed in an ultrahigh vacuum (UHV) system (base pressure 5×10^{-10} Torr) facing an annular extraction anode and a phosphor screen. Upon the application of a sufficient negative voltage to the tip, V_{FE}, electrons are emitted from its apex and accelerate toward a screen several centimeters away, thus forming the FEM pattern. The FEM pattern is a projected image of the apex emission zone magnified by up to 10^6 in which the features with the lowest radius of curvature are strongly enhanced. The image is a view of the top of the tip apex or the CNT cap, with intensities depending on their relative rates of electron emission. One important aspect of this projection geometry is that if the emitter is tilted the corresponding FEM pattern translates on the screen (like moving your aim with a flashlight), while if the pattern rotates as a whole the only physical possibility is that the emission zone physically rotates about its axis. The W tip emission area has a radius $r_W \sim 60$ nm, which sets the scale of the system. The W tips are first covered in situ with a graphite diffusion barrier by heating in acetylene at a pressure of $P_{C_2H_2} \sim 1 \times 10^{-4}$ Torr. Ni is then deposited on the tip and formed into nanoparticles by dewetting (Figure 2a). CNTs were then induced to grow directly on the Ni nanoparticles by CVD in acetylene at 800 °C during FEM imaging. We use acetylene pressures, $P_{C_2H_2}$, in the $(1-2) \times 10^{-7}$ Torr range during growth, lower than values found in the literature. A film depicting the process is available as Supporting Information.

A sequence of photos from one of the growth experiments is shown in Figure 2. The first pattern (Figure 2a) corresponds to the emission from the Ni particles just before growth. V_{FE} was -1600 V. Each roughly round spot is due to emission from one Ni nanoparticle. The sizes of these nanoparticles are difficult to estimate accurately because the local fields magnify their FEM images:[11] our separate TEM studies showed they are 1−20 nm in diameter, similar to those used for in situ TEM growth. In general, the CNT nucleation occurs about 2−3 min after introduction of acetylene. One bright spot suddenly appeared from one video frame to the next (Figure 2, panels a to b) meaning a CNT had nucleated at the Ni particle in 40 ms or less. The nucleation varied from abrupt to very gradual for different CNTs. As the CNT lengthened the CNT FEM pattern intensified due to the strengthening of the cap electric field and its diameter increased due to the weakening of the forward focusing effect of the base W tip (Figure 2, panels c and d). We progressively decreased V_{FE} to maintain a relatively constant intensity on the screen, thus avoiding current-induced destruction of the CNT. During this run we decreased V_{FE} stepwise starting from -1600 to -200 V by the end of growth while the pattern diameter expanded 5-fold (Figure 3a). As we discuss next, this comportment can only be explained by the progressive formation of a nanometric size cylindrical object at the Ni nanoparticle, directed radially from the W tip apex. Below we show strong proof that these objects are CNTs and often SWNTs. We have not yet succeeded in transferring one of these delicate samples to a TEM for detailed structural characterization, including side view, atomic-scale imaging of the CNTs.

Simulations of the electrostatic potentials and electron trajectories of this system have been made as a function of CNT length L to show that the measurements are consistent with a nanocylinder geometry and to estimate the final length of this nanotube. Zoom views of the simulations near the nanotube for one set of parameters are depicted in Figure 3a. Care has been taken to include all the elements of the macroscopic tip and interelectrode distances in the simulation (not shown) which must be accurate over a large range of length scales (sub-nanometer to centimeter). To first order V_{FE} for constant current scales with ϕ/L, where ϕ is the nanotube diameter, while the pattern diameter, ϕ_P, scales with L. However, second order corrections due to the entire electrostatic environment must be included if the simulations are to approach a quantitative description of V_{FE} and ϕ_P. As an example results for a (24,0) SWNT ($\phi = 1.88$ nm) of varying length are plotted with the data in Figure 3b (red curve) with the only assumption being a constant growth rate G and $r_W = 60$ nm for the carburized W base tip. There is excellent agreement between the simulations as a function of CNT length and the measured V_{FE} for $G = 0.08$ nm/s. This gives a final length of $L = 60$ nm. These values of G and L depend roughly linearly on the choice of ϕ for which we do not have an independent measure at this point (see below). However in Figure 3b is also shown the calculated expansion of the pattern as a function of length using the same ϕ and G. There are no free new parameters, and the fit is satisfactory confirming that a reasonable choice of ϕ was made. A better fit would need a better knowledge of many second order effects that come into the calculation: exact substructure of the W tip, specific FE tunneling calculation for the nanometer size cap, etc. In the absence of a confirming TEM image, one could argue that the patterns

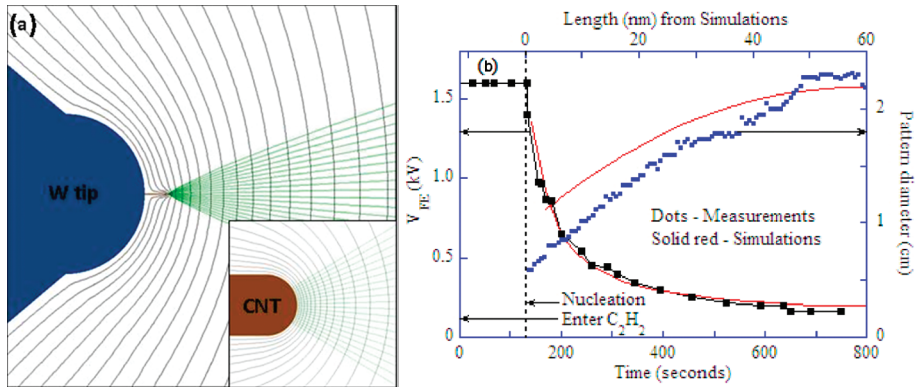

Figure 3. (a) Simulations of the electrostatic potentials and electron trajectories in the near apex region. The total system is much larger and includes the tip mounting structure and extraction anode. The sharp, short section is the nanotube on the tip apex. Inset: Zoom of the simulation at the nanotube apex. (b) Decrease in V_{FE} during growth to maintain constant image intensity on the screen and increase in the pattern diameter (see text). The solid red lines are the result of electrostatic simulations assuming a constant growth rate of 0.08 nm/s.

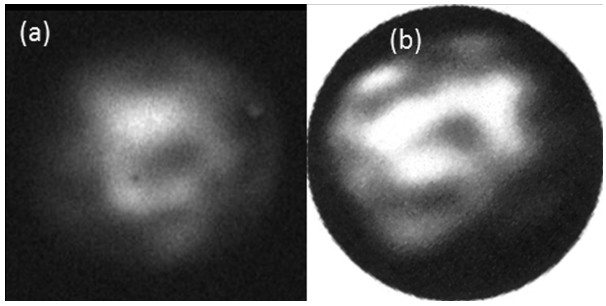

Figure 4. (a) A CNT FEM pattern from this work. (b) FEM pattern obtained by K. A. Dean et al.[13] from a SWNT. Both are at room temperature, which gives a higher definition in the FE pattern than at the growth temperature of 800 °C due to reduced transverse tunneling.

are due to the growth of "something else" such as a nanomountain slowly forming on the base tip. We have also simulated the case of a cone terminated by a partial sphere. Without going into the details, neither the voltage nor the size of the pattern can come close to fitting our experiments.

A strong indication that we are actually growing SWNTs is the striking similarity of one of our FEM patterns with one obtained previously for SWNTs[13] (see Figure 4) which were supported by first principle calculations.[14] Blind comparisons of the voluminous literature of FEM patterns confirmed that this type of pattern is absolutely unique, like a fingerprint, and resembles only our FEM patterns. A perfect match cannot be expected because there are many hundreds of different cap structures which would each have a specific pattern.[14] Note that electrostatic simulations gave $G = 0.07$ nm/s for this nanotube, close to G for the first CNT.

After these preliminaries we now turn to a case where, in addition to the increase in pattern size and decrease in applied voltage, the FEM pattern made ~180 axial revolutions during a growth. A sequence of photos during one revolution is presented in Figure 5a. Unlike the growth of Figure 2 this CNT cap and corresponding FEM pattern were not uniform, thus providing the necessary contrast to observe the rotation. The rotation is quite striking in the video film (see video in the Supporting Information) as compared to the still photos in Figure 5a. It is reminiscent of the rotation that was observed by Dean et al.[15] during the progressive destruction of a CNT ring by ring by high-current-induced-heating during FEM, the possibility of which was discussed originally by Rinzler et al.[16] A large part of the video was analyzed by both visual inspection and numerical analysis which gave the same results. The visual analysis is in Figure 5b showing a steady increase in the angle associated with regular rotations with an average period of 3.5s. The only factor that can drive such a rotation is the insertion of C-atoms as they dock to the kinks on the edge of a chiral tube (insert Figure 5b). This corresponds to the recently proposed screw dislocation (SDL) model[10] that draws on earlier work on crystal growth.[9] Growth rate, G, and length, L, of the nanotube can be immediately estimated using the unit cell (a hexagon) height of 0.21 nm, corresponding to one row of hexagons being added upon completion of each full revolution. One gets $G \sim 0.21/3.5 = 0.07$ nm/s and total length $L \sim 180 \times 0.21$ nm $= 38$ nm, in excellent agreement with the estimates by electrostatic calculations for the nanotubes above. The rotation was regular for the first half of the growth but became more and more erratic as the end of the growth approached. It even reversed several times by a large fraction of a single turn (Figure 5b). However the intensity still increased showing the nanotube was still growing. This could be explained by the appearance of defects in the structure that reverse the helicity, e.g., an insertion of a 5/7 defect can induce the change $(n,1) \rightarrow (1,n)$ and thus reverse the direction of rotation. This is reminiscent of the decrease in G observed previously[6] in which a progressive poisoning of the catalyst was suggested.

To go further in the analysis of the rotation, a slice of the video, chosen arbitrarily near the middle of the growth of the nanotube that represented 5.5 rotations, was examined frame by frame (see video in the Supporting Information). The analysis is shown in Figure 6. The rotation actually proceeds by discrete steps lasting 1−14 frames with about ~24 steps for each revolution (i.e., 25, 25, 22, 21, 25) and an average step size of five frames (0.2 s). The immediate conclusion is that we are observing the growth of a CNT atom by atom and that we can count the number of atoms on its circumference. Some steps of less than 1 video frame

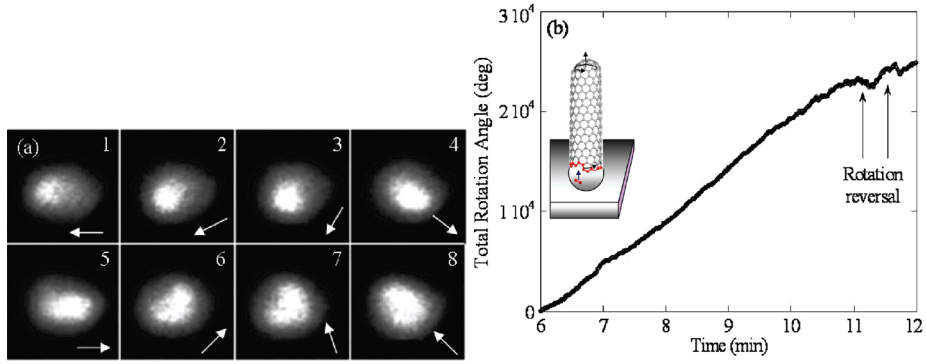

Figure 5. (a) Sequence of FEM patterns from a growing CNT that follows a single revolution as the CNT lengthens (in the order 1 to 8). (b) Angle of the pattern as a function of time during a large part of the growth.

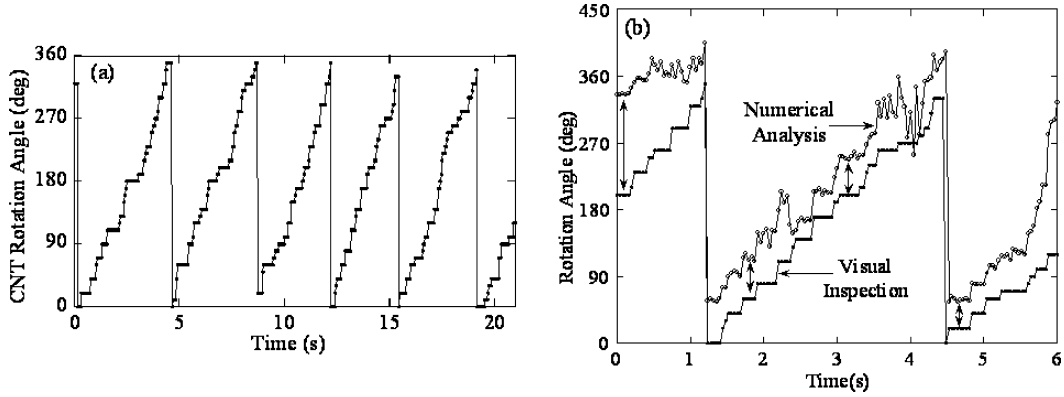

Figure 6. (A) Frame by frame measurement of the rotation angle of the pattern showing that it proceeded step by step. The number of the steps for the five cycles are (25, 25, 21, 21, 25) varying because rotations over one or less frames are difficult to tabulate. (B) Detail of the fourth cycle with 21 steps in the cycle. The numerical image analysis has been displaced by 60° for clarity.

could be missed in the counting, but large jumps in the angle versus time curves of Figure 6 were not observed. The histogram of step lengths fits roughly a Poisson distribution within this rather narrow statistical sample with a maximum at one frame. No obvious correlation between step lengths and angle has as yet been detected. The steps were first determined by visually following the images frame by frame with a protractor on the screen which gave an excellent definition of the steps. Numerical image analysis was also carried out with a program that first determined the intensity center in each image and then fitted the pattern to an ellipse. This is less effective because of the noise and poor resolution of the video which meant that the program missed some steps, particularly those of few frames. Nevertheless Figure 6b shows an excellent overall agreement between the two methods. 24×2 atoms would correspond to a diameter of $ø = 1.88$ nm for a nearly (24,0) zigzag SWNT (or more precisely a chiral (23,1)). It has been pointed out for some time that from a theoretical point of view it is energetically favorable to attach dimers as opposed to monomers[17−19] (the primitive cell contains two atoms) but until now there was no experimental evidence for this. The rarity of SWNTs with $\phi < 1$ nm in CVD growth, particularly on Ni under similar conditions,[6−8] argues against growth by monomers, though a more direct proof of this is desirable. In summary, the FEM observations place the sizes of these CNTs in the low nanometer range, the number of steps per revolution is very regular, their number accords with SWNT circumferences and the FEM images agree with SWNT images in the literature. As well, low pressures and high temperatures with C_2H_2 and Ni nanoparticle catalysts have been shown to favor the growth of small diameter CNTs particularly SWNTs.[20] Taking this all together we conclude that each step marks the integration of a single carbon dimer into a SWNT.

The Ni particle formation and CNT growth procedures are yet to be optimized, which is often a long and arduous task. For these experiments the growth statistics were as follows: 15 successful growths (for 33 runs) of which four rotating growths, six nonrotating growths, and five growths with FEM patterns at the screen edge where rotation could not be determined. Note that at these high temperatures FEM patterns blur, and if the cap is too uniform or the image too saturated, a rotation may not be visible. Thus some or all of the six growths classified nonrotating may actually have rotated. Also an armchair SWNT would not rotate. The three other rotation growths were not nearly as regular. Interspersed with regular rotation sequences, there were often sudden rotations over larger angles in single frames and faster increases in emission current associated with faster CNT elongation. This can be the consequence of different SWNT helicity but may also be related to the specifics of the Ni nanoparticle or the video camera not being fast enough to capture all the plateaus. A final point is that the FEM patterns have quite constant forms during growth which strongly suggests that this is root growth and not tip growth in agreement with all in situ TEM studies of SWNTs.[6−8]

The growth rates G were quite uniform during each growth (see Figures 3a and 6b) and from run to run (0.08−0.07 nm/s) and are lower than other reported values. This permits a more active use of external control parameters. For example the low G is likely related to our very low $P_{C_2H_2}$, which is much less than most of the TEM studies (10^{-3}−10^{0} Torr)[5,7,8] except one[6] at 4×10^{-6} Torr. This last is only 20× higher than our $P_{C_2H_2}$ and had the previously lowest G after nucleation of 0.1−0.3 nm/s. It has been argued that the rate-limiting step at 10^{-3} Torr was the carbon diffusion over the Ni catalyst[5] and was a combination of diffusion and pressure[6] at 4×10^{-6} Torr. Here we may have crossed over into a regime where pressure dominates G. The kinetic theory of gases gives an arrival rate of 160 C_2H_2 molecules/s on 1 nm^2, which is within a factor of 20 of our G of 14 atoms/s. As for temperature we were able to restart the growth of Figure 2a near the end by simply boosting the temperature by 50 K, which is an example of how one can vary this parameter interactively.

Along with positioning strategies, the community seeks to achieve a level of control of CNT growth that predetermines helicity, diameter, length, quality, and number of tubes, thus predetermining their physical properties. A general scheme for catalytic growth was already proposed by Baker for the growth of hollow carbon fibers,[21] but ultimately one needs knowledge and control achieved for molecular beam epitaxy (MBE)[22] where the atomic seed lattice orients the rest of the growth. Thus measurement techniques, models, and control are needed at the atomic scale as this is the size of the critical growth zone. Simulations suggest such models,[3,4] but the many possibilities they open need to be guided by simpler principles and experiment. The SDL mechanism[10] is similar to MBE in that it means adding atoms sequentially around the already formed edge of the CNT. An experimental method that can measure growth with an atomic resolution is needed to test this theory and find the experimental conditions over which it is applicable. This in situ FEM growth provides such a method. The atom by atom FEM observations are reminiscent of the use of reflection high energy electron diffraction (RHEED) for MBE which allowed essential studies of monolayer by monolayer growth.[23,24]

We propose that the SDL mechanism[10] controls an important proportion of our growths. Though not discussed in the original model, it surprisingly manifests itself by driving the rotation of the whole SWNT body by the insertion of dimers. This scheme implies that there must be both longitudinal and rotational sliding between the nanoparticle and edge of the CNT in order to give space to the newly accreted carbon dimers. Relative longitudinal movement is consistently observed in TEM observations of growth of CNTs[5−8] but not axial rotation.

In conclusion this article brings new insights to the three elements needed for advancing controlled CNT growth: measurement, model, and control. The striking observation by FEM of the fabrication atomic brick by atomic brick of a molecular system is a new measurement technique at the atomic scale, the rotation lends strong support that SWNTs can grow by the SDL model, and the slow and regular growths suggest that pressure and temperature can become interactive control parameters. This work does not exclude other growth mechanisms particularly for MWNTs and for more complicated growths that integrate numerous defects (e.g., ref 5). However it appears to us to be the most basic, and proving its existence is of primary importance for understanding other growths. This is the first experimental support that SWNT growth proceeds by the insertion of dimers, though this must be confirmed. Many new questions for theory and experiment are now posed such as how exactly the atom insertion generates the rotation with perhaps a particular defect on the catalyst[25] acting as a fulcrum, what is the mechanism here that stops the growth and how can it be extended, and finally can the SDL model be exploited as a seed method for controlling CNT parameters such as helicity?

"*E pur si muove*", Galileo (And yet it does turn).

Acknowledgment. This work was carried out within the framework of the Group Nanowires-Nanotubes Lyonnais. The authors wish to thank H. Ayari for the numerical analysis and the program PNANO of the Agence National de Recherche (Français) for financial support. B.I.Y. was supported by the National Science Foundation and the US Air Force Research Laboratory.

Supporting Information Available: (1) A video animation that depicts the process of combined field emission and growth to help readers that are unfamiliar with the field emission geometry to better see (2) the rotations of the CNT, a video film mentioned in the text, which contains the leading result of the article. This video shows 5.5 rotations over a time of 18 s selected randomly from the 12 min growth. The counting of rotations is as easy as counting the turning of the hand of a clock, and because the video is timed, this is how we measure the rotation speed. As well, by just stepping through the film anyone can clearly see the step-by-step rotation. (3) A final file (pdf) shows how the film was analyzed for measuring the discrete nature of the rotation shown in Figure 6.This material is available free of charge via the Internet at http://pubs.acs.org.

References

(1) Saito, R.; Dresselhaus, G.; Dresselhaus, M. S. *Physical Properties of Carbon Nanotubes*; Imperial College Press: London, 1998.
(2) Loiseau, A.; Launois, P.; Petit, P.; Roche, S.; Salvetat, J.-P. *Understanding Carbon Nanotubes: From Bacis to Applications*; Lectures Notes in Physics 677; Springer: Berlin, 2006.
(3) Gavillet, J.; Loiseau, A.; Journet, C.; Willaime, F.; Ducastelle, F.; Charlier, J.-C. *Phys. Rev. Lett.* **2001**, *87*, 275504.
(4) Amara, H.; Bichara, C.; Ducastelle, F. *Phys. Rev. Lett.* **2008**, *100*, 056105and references therein.
(5) Helveg, S.; López-Cartes, C.; Sehested, J.; Hansen, P. L.; Clausen, B. S.; Rostrup-Nielsen, J. R.; Abild-Pedersen, F.; Nørskov, J. K. *Nature* **2004**, *427*, 426.
(6) Lin, M.; Pei Ying Tan, J.; Boothroyd, C.; Loh, K. P.; Tok, E. S.; Foo, Y.-L. *Nano Lett.* **2006**, *6*, 449.
(7) Hofmann, S.; Sharma, R.; Ducati, C.; Du, G.; Mattevi, C.; Cepek, C.; Cantoro, M.; Pisana, S.; Parvez, A.; Ferrari, A. C.; Dunin-Borkowski, R.; Lizzit, S.; Petaccia, L.; Goldoni, A.; Robertson, J. *Nano Lett.* **2007**, *7*, 602.
(8) Yoshida, H.; Takeda, S.; Uchiyama, T.; Kohno, H.; Homma, Y. *Nano Lett.* **2008**, *8*, 2082.

(9) Burton, W. K.; Cabrera, N.; Frank, F. C. *Nature* **1949**, *163*, 398.
(10) Ding, F.; Harutyunyan, A. R.; Yakobson, B. I. *Proc. Natl. Acad. Sci. U.S.A.* **2009**, *106*, 2506.
(11) Gomer, R. *Field Emission and Field Ionization*; Harvard University Press: Cambridge, 1961.
(12) Bonard, J.-M.; Croci, M.; Conus, F.; Stöckli, T.; Chatelain, A. *Appl. Phys. Lett.* **2002**, *81*, 2836.
(13) Dean, K. A.; von Allmen, P.; Chalamala, B. R. *J. Vac. Sci. Technol., B* **1999**, *17*, 1959.
(14) Khazaei, M.; Dean, K. A.; Farajian, A. A.; Kawazoe, Y. *J. Phys. Chem.* **2007**, *111*, 6690.
(15) Dean, K. A.; Burgin, T. P.; Chalamala, B. R. *Appl. Phys. Lett.* **2001**, *79*, 1873.
(16) Rinzler, A. G.; Hafher, J. H.; Nikolaev, P.; Smalley, R. E. *Science* **1995**, *269*, 1550.
(17) Saito, R.; Dresselhaus, G.; Dresselhaus, M. S. *J. Appl. Phys.* **1993**, *73*, 494.
(18) Maiti, A.; Brabec, C.; Roland, C.; Bernholc, J. *Phys. Rev. Lett.* **1994**, *73*, 2468.
(19) Charlier, J.-C.; De Vita, A.; Blase, X.; Car, R. *Science* **1997**, *31*, 647.
(20) Sharma, R.; Rez, P.; Brown, M.; Du, G.; Treacy, M. M. J. *Nanotechnology* **2007**, *18*, 125602.
(21) Baker, R. T. K.; Harris, P. S.; Thomas, R. B.; Waite, R. J. *J. Catal.* **1973**, *30*, 86.
(22) Cho, A. Y.; Arthur, J. R. *Prog. Solid State Chem.* **1975**, *10*, 157.
(23) Neave, J. H.; Joyce, B. A.; Dobson, P. J.; Norton, N. *Appl. Phys. A: Mater. Sci. Process.* **1983**, *31*, 1.
(24) Purcell, S. T.; Heinrich, B.; Arrott, A. S. *Phys. Rev. B* **1987**, *35*, 6458.
(25) Zhu, H.; Suenaga, K.; Hashimoto, A.; Urita, K.; Hata, K; Iijima, S. *Small* **2005**, *1*, 1180.

NL901380U